

ON THE AHMED BODY WAKE

Václav Uruba, Ondřej Hladík
Institute of Thermomechanics AS CR, v.v.i., Praha

Abstract

The Ahmed body is now accepted as a test-case prototype of a typical modern passenger car possessing all typical aerodynamic features – a bluff body with separated boundary layer generating wake resulting into pressure drag. Several types of vortical structures arise in the wake, quasi-stationary and highly dynamic in nature.

In the presented paper both stationary and dynamical behaviour of structures in wake is studied. Two configurations with slant angles of 25 deg and 35 deg are considered as the test-cases.

The small variant model of Ahmed body, scale 3/20 relative to original Ahmed body defined in Ahmed (1989) is subjected to experimental study, mean flow velocity about 7 m/s resulting in Reynolds number 54 thousands.

The stereo time-resolved PIV technique is used for the wake transversal section monitoring 0,1 model length distance, the 1000 instantaneous pictures with frequency 500 Hz have been acquired. Preceding studies Uruba (2009) and Uruba, Sedlak (2009) analysed flow in the wake in longitudinal plane of symmetry only.

The Proper Orthogonal Decomposition (POD) technique is used for the dynamical data analysis (see e.g. Uruba, 2009).

1. Introduction

Several researchers have worked on the experiments and numerical modeling of the flow over so-called Ahmed body. To develop turbulence models for complex geometry cases, a simplified car model, known as the Ahmed body, has been tested by Ahmed and his coworkers in the early 1980s – see Ahmed (1981), Ahmed (1983) and Ahmed and Ramm (1984). The Ahmed body is made up of a round front part, a moveable slant plane placed in the rear of the body to study the separation phenomena at different angles, and a rectangular box, which connects the front part and the rear slant plane, as shown in Figure 1. All dimensions listed in the figure are in mm.

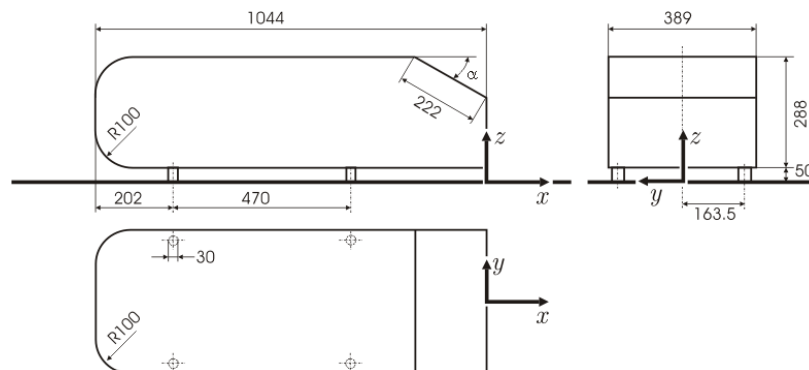


Fig. 1 – The original Ahmed body

Two configurations with slant angles α of 25 deg and 35 deg are considered as the test cases. For this configurations detailed LDA measurements have been performed by Lienhart and Becker (2000) in the low-speed wind-tunnel with a cross-section of $1.87 \times 1.4 \text{ m}^2$ (width x height) with a bulk velocity of 40 m/s. The test-section of the wind-tunnel was 3/4 open (only ground plate present). In the experiment perform by the Ahmed, flow velocity was taken 60 m/s, Reynolds number was 4.29 million based on model length.

The Ahmed body wake is subject of many experimental and numerical studies. A few important qualitative results on the wake structure will be shown now. In general, the wake consists of systems of vortical structures.

In the Gilliéron, Chometon (1999) the vortex wake system takes the form of two counter-rotary lateral vortices (T) starting at a separation line AB, and we observe an open separation bulb, D, located at the upper part of the rear window. The fluid inside the separation bulb experiences a rotary motion (centred around point A) that generates two singular points, S1 and S2. The base flow combines with the rear window flow to generate a detachment node N2. At the base surface, the converging toroid streamlines generate a singular point in the form of an attachment node, identified as N1.

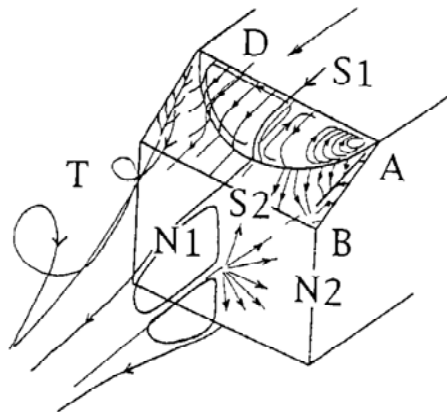


Fig. 2 – Schematic view of the wake structure close to the body (figure by Gilliéron, Chometon, 1999)

Franck & D'Elía (2004) describe the far wake structure as follows (see Fig. 3). The slant and the vertical base of the rear end have edges that allow the formation of vortices by a rolled up of the shear layer. The side edges create a longitudinal vortex indicated in figure as C and the top and bottom edges of the vertical base create two recirculatory flows A and B situated one over the other. Experimental evidence does not indicate that these two flow regions end on the base surface; therefore these two recirculatory flow may seem to have been generated through two horseshoes vortices located one over the other in the separation bubble indicated as D, those vortices determine a singular point N.

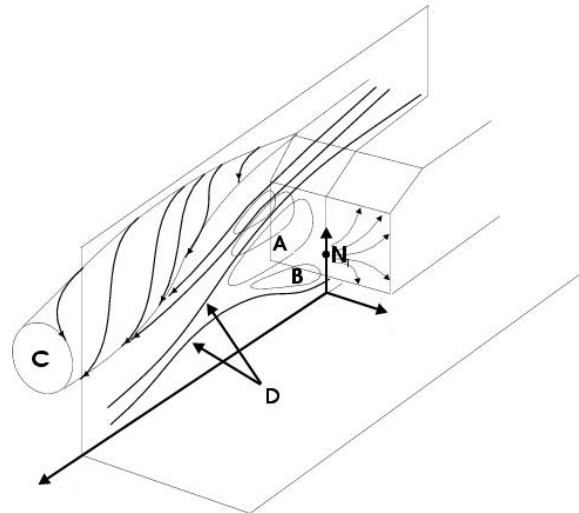


Fig. 3 – Far wake structure (from Franck & D'Elia, 2004)

Influence of the slant angle on the wake structure is studied as well. The URANS simulations by Ceyrowsky et al. (2009) show the overall structure of the wake for the two cases characterized by the slant angles of 25 deg and 35 deg – see Fig. 4.

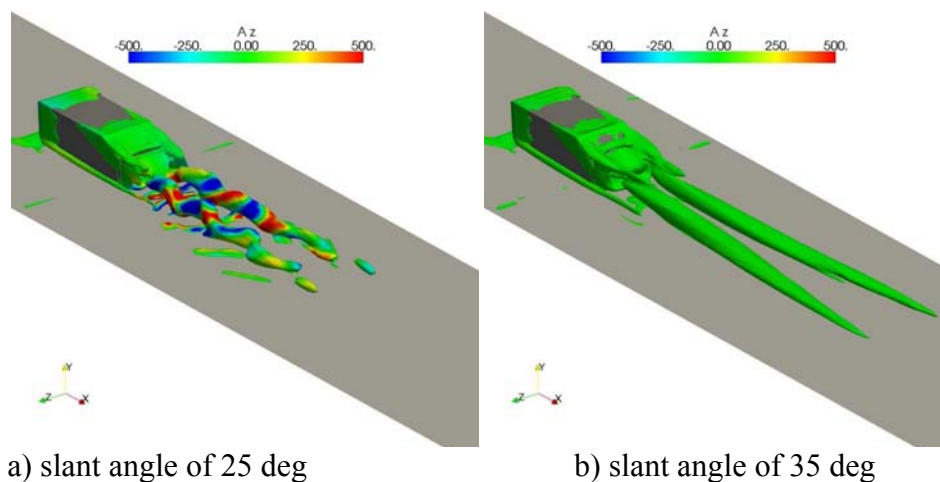


Fig. 4a,b – Wake vortices visualised using Q-criterion (URANS simulation by Ceyrowsky et al., 2009)

The Fig. 4 indicates unstable behaviour of the longitudinal vortices, however it is not sure whether this behaviour is connected with physical nature of the phenomenon or rather with numerical instability of the mathematical model. For the 25 deg case the separation and reattachment of the roof boundary layer on the slant is indicated, which could be of nonstationary nature. In the 35 deg case no reattachment occur, in general.

There is still lack of experimental data concerned dynamics of the Ahmed body wake.

2. Experimental setup

Our model was placed in the open test section in the tunnel exit 250 x 250 mm², flow velocity 6.5 m/s, blockage was about 8 %. The model was geometrically similar to

the original Ahmed body in side view, the ratio 3 : 20 meaning that length of our model was 156.6 mm. Reynolds number was by 2 orders lower than in original Ahmed case, actual value $Re = 54\ 000$.

The time-resolved stereo PIV method was used for the experiments. The measuring system DANTEC consists of laser with cylindrical optics and two CMOS cameras. The software Dynamics Studio 2.2 was used for velocity-fields evaluation. Laser New Wave Pegasus Nd:YLF, double head, wavelength 527 nm, maximal frequency 10 kHz, a shot energy is 10 mJ for 1 kHz (corresponding power 10 W per head). Two cameras NanoSense MkIII, resolution 1280 x 1024 pixels and frequency 500 double-snaps per second, 1000 double-snaps were acquired in sequence corresponding to 2 s of the record time.

Measuring plane was perpendicular to the main-flow 0.1 of the Ahmed body length downstream the body rear part. The stereo-PIV configuration with cameras angle 40 deg relative to the body symmetry plane was used with the Scheimpflug condition satisfied. The situation is shown in Fig. 5.

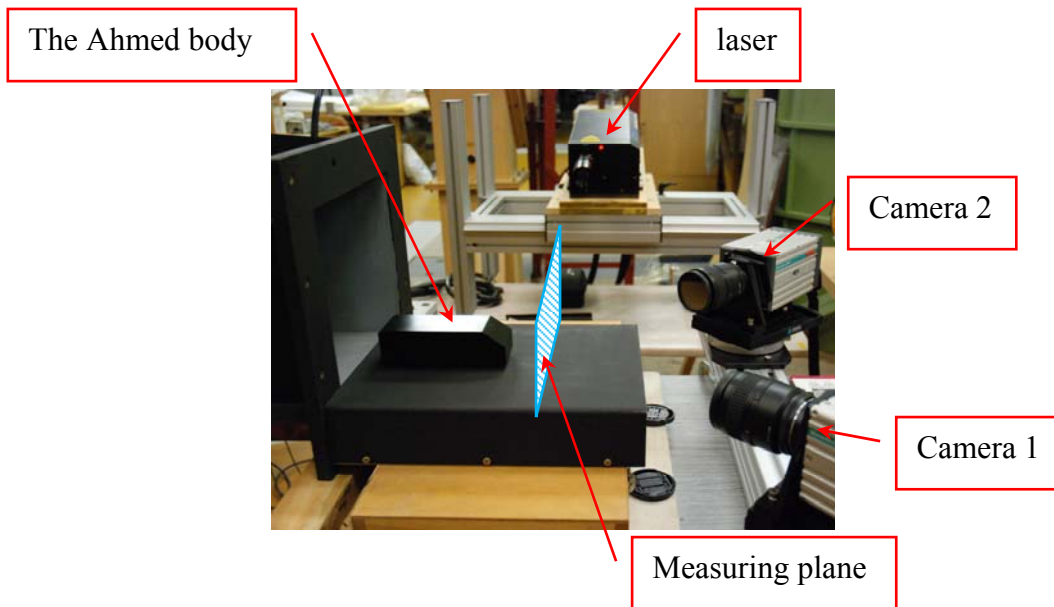


Fig. 5 – Experimental setup

The origin of the coordinate system was placed to surface in the body symmetry plane, which is defined by yz axes, while x axis is perpendicular. Thus, x and y axes are transversal, while z axis is longitudinal relative to the main flow, x axis in wall, y perpendicular to the wall.

3. Results

A standard DANTEC procedure for evaluation of 3 velocity components in measuring plane was applied. In the first phase of the study mean values and statistical moments, then the Proper Orthogonal Decomposition (POD) method was applied on velocity fluctuation fields.

The results are shown as vector and scalar fields, the two slant angles mentioned above were being compared. The mean velocities U , V and W stand for the components

in x , y and z directions respectively. Sometimes vector-lines are added for U and V velocity components.

3.1 Mean flow

First, the mean vector fields were evaluated from the acquired data. In Fig. 6 all 3 mean velocity vector components are shown for the two cases. The U and V mean velocity components are shown as in-plane vectors, while W component is shown as a scalar field by colour. The Ahmed body silhouette is shown as well.

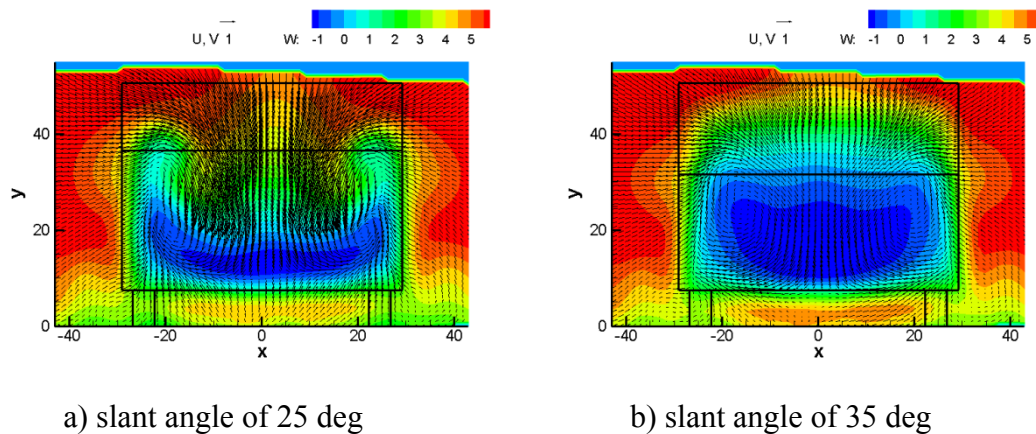


Fig. 6a,b – Mean velocity vector-fields

The 25 deg case shows very strong down-flow in vicinity of the plane of symmetry and relatively weak contra-rotating vortex pair, while the 35 deg case exhibits much stronger vortices (shown with help of vector-lines). The size of the back-flow region (in blue) differs considerably for the two cases in question, for the 35 deg case is much bigger.

To see better structure of the wake the vector-lines were added in Fig. 7.

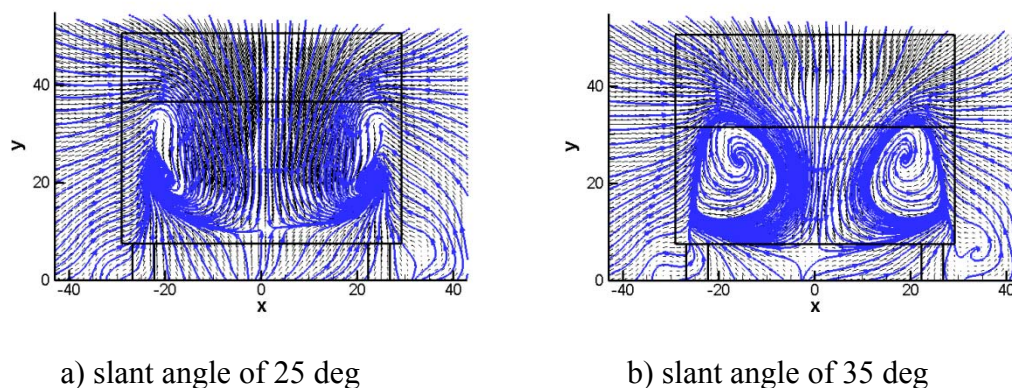


Fig. 7 – Mean velocity vector-fields with vector-lines

The Fig. 7 shows clearly size of the counter-rotary lateral vortices. They are much bigger in the 35 deg case. This effect is even clearer for the in-plane vorticity.

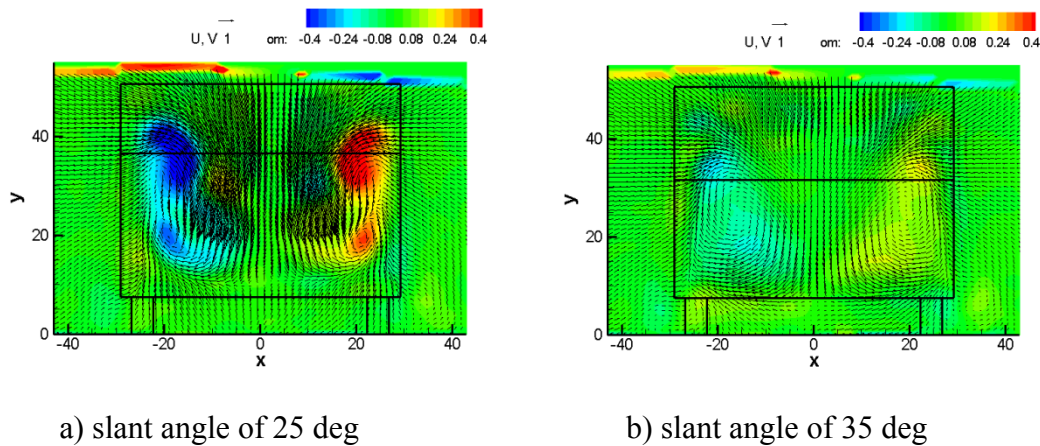


Fig. 8 – In-plane mean vorticity distributions

Fig. 8 shows that the vorticity is much higher in the 25 deg case even though the vortices are smaller.

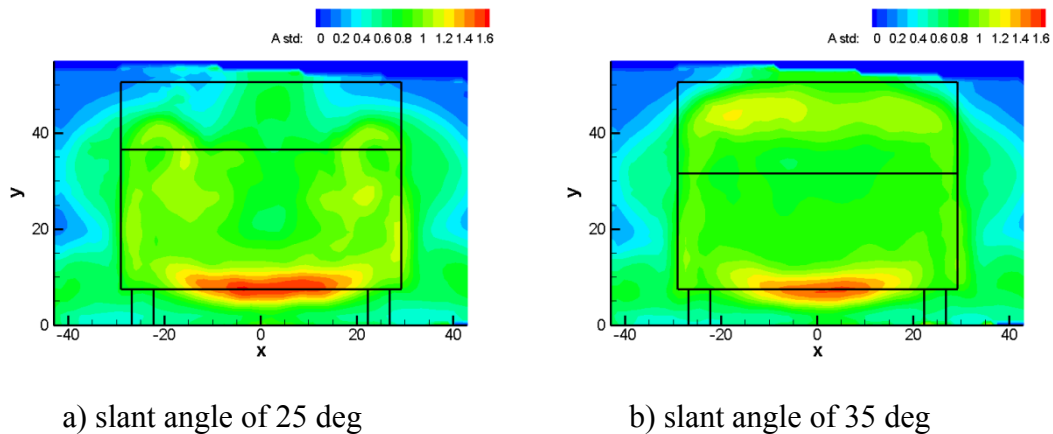


Fig. 9 – Velocity standard deviation distributions

Fig. 9 represents distribution of the velocity standard deviation taking into account all 3 velocity components. This value corresponds to square root of the turbulent kinetic energy (TKE). We could recognize the most intense turbulent activity near the bottom edge of the Ahmed body. The secondary maxima could be recognized for the case of 25 deg slant angle near the side contour, especially close to rear edge corresponding to position of the longitudinal vortices. In the case of 35 deg slant angle the secondary maximum of turbulent energy is located close just below roof level.

3.2 Fluctuations

Then, the mean vector field is subtracted from each instantaneous velocity field and the fluctuations are subjected to further analysis.

The POD modes have been evaluated for both cases. In Fig. 10 Energy content of the modes is relatively low – the first mode contains only 5 % of the total turbulent kinetic energy (TKE) and first 100 modes contain only about 70 % TKE.

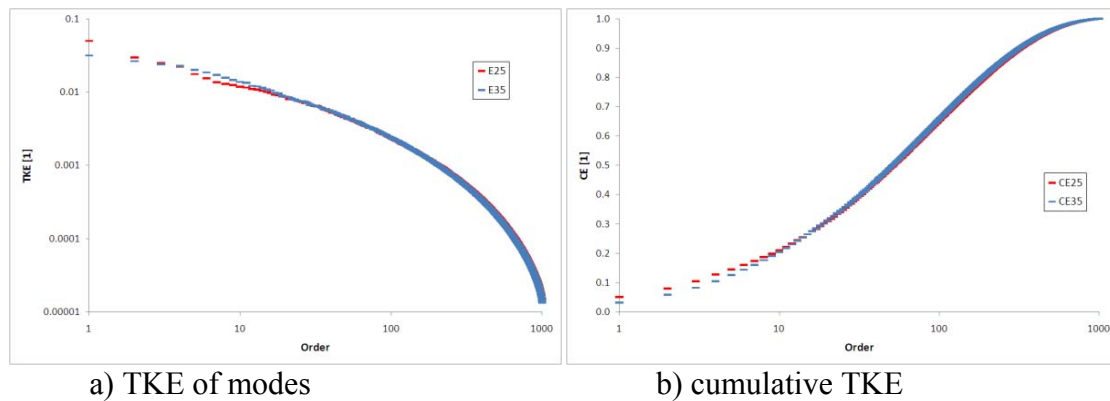


Fig. 10 – Energy content of POD modes

The spectra of chronoses in Fig. 11 suggest that there is a very distinct frequency in the 25 deg case on approx. 50 Hz connected with 1st and 2nd modes. Then, the corresponding toposes represent two phases of the quasiperiodical dynamical process in the wake, shifted by $\pi/2$.

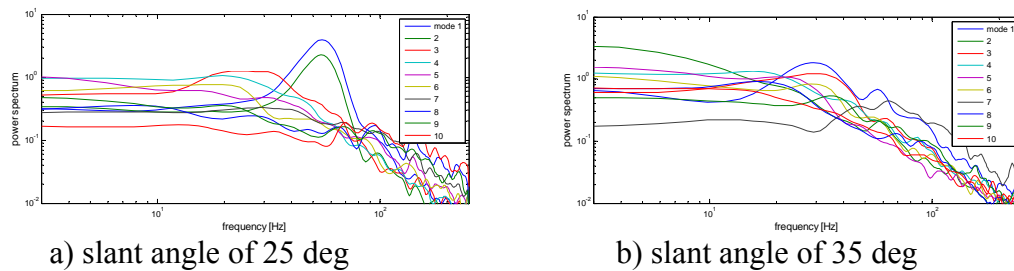


Fig. 11 – Energy spectra of first 10 POD modes

These modes represent activity of flow from the body bottom, the 1st mode includes 2 distinct vortices. However, the two first modes for the 25 deg case contain only about 8 % of the total TKE. Part of the corresponding chronoses time-series is given in Fig. 12.

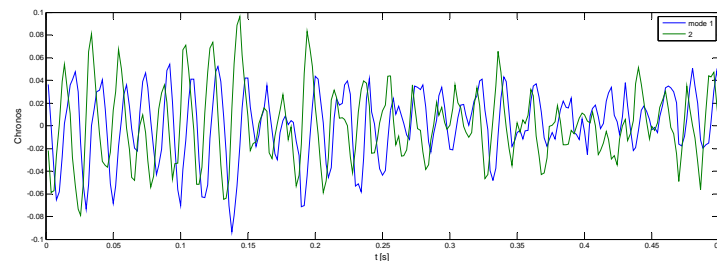
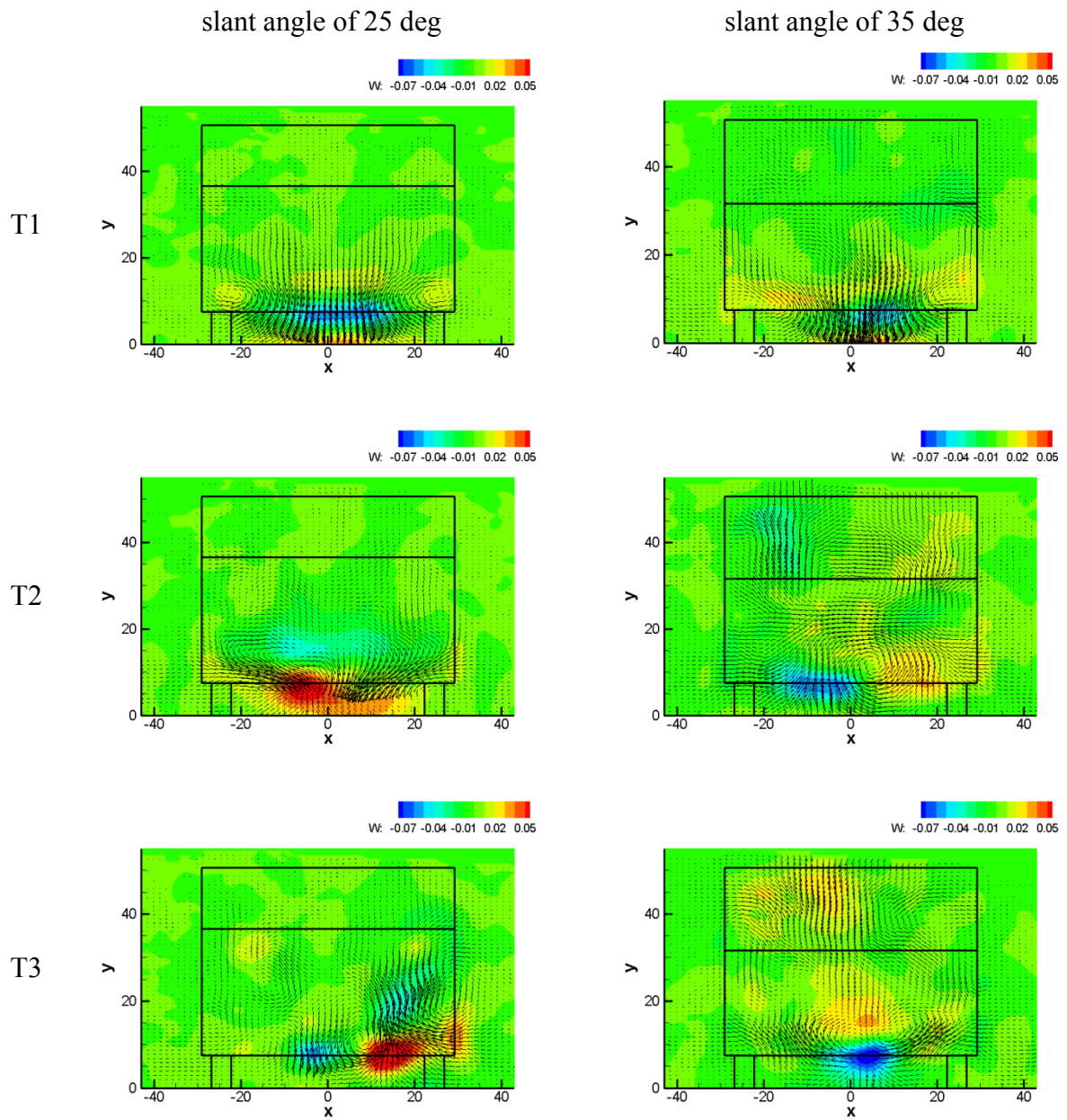
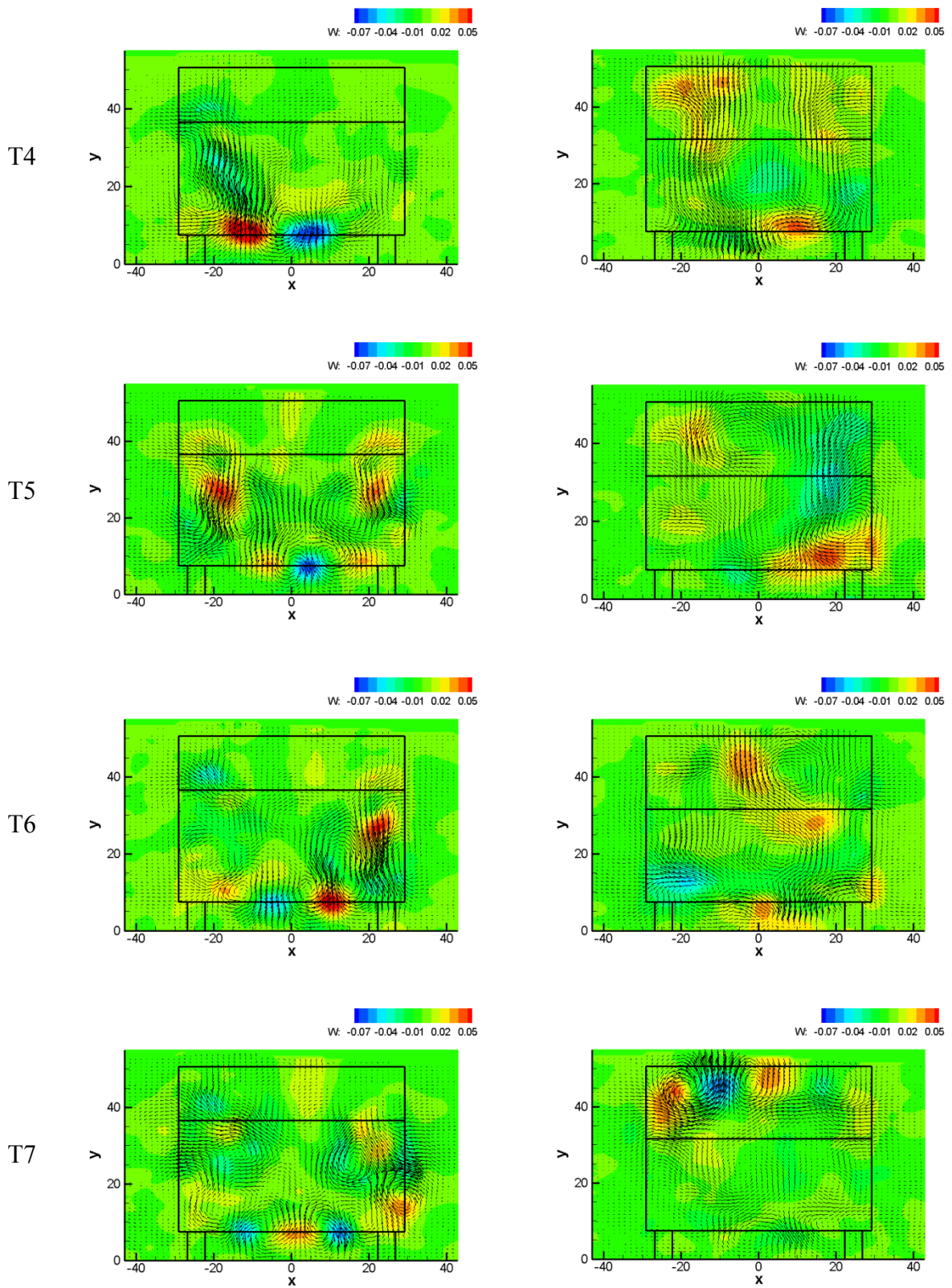


Fig. 12 – First 2 chronoses for slant angle of 25 deg case

All other spectra indicate broad-band processes without any distinct frequency peak. The other toposes consist of vortical structures, nodes and saddle points, they are similar to those evaluated from the flow in the plane of symmetry (see Uruba, 2009).





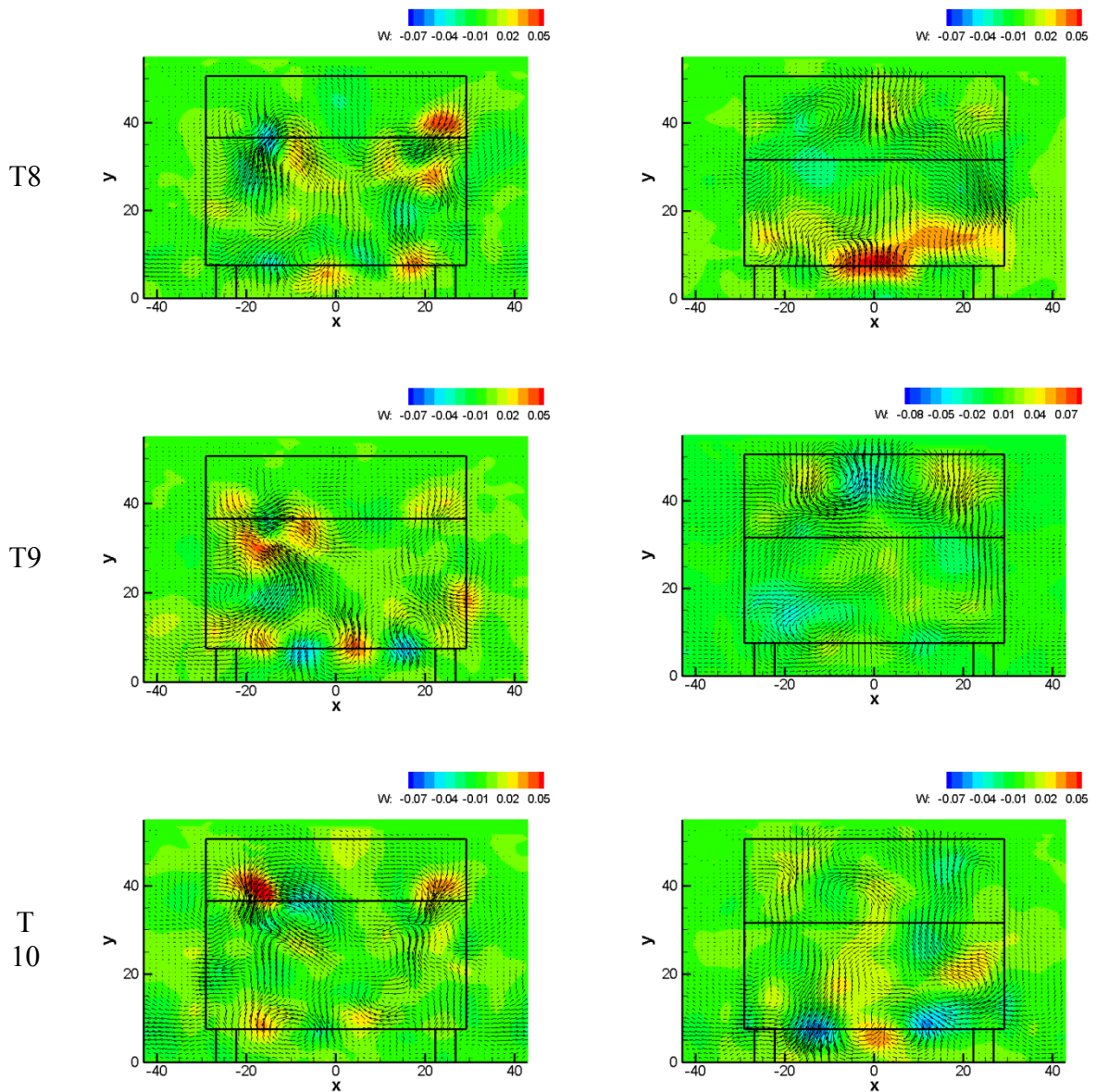


Fig. 13 – First 10 toposes

In Fig. 13 there are the first 10 toposes for both cases in question. Rows correspond to a topos number, left column for the slant angle of 25 deg case and right column for the 35 deg case.

The mode energy and entropy distribution have been studied as well, see Figures 14 and 15. The mode energy distribution follows the turbulent kinetic energy distribution shown in Fig. 9. Entropy represents coherency of the local velocity time evolution or convergence rate of the modes, the value 1 corresponds to totally incoherent case with homogeneous energy distribution between modes, while 0 is perfectly coherent case with all energy concentrated in the first mode. Positions of the local entropy minima (i.e. maximal coherence) correspond more or less to those of energy maxima.

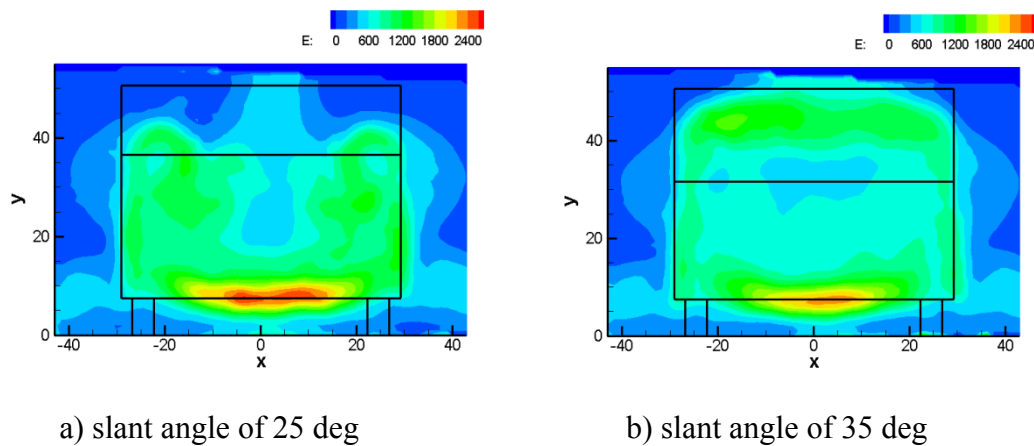


Fig. 14 – POD energy distribution

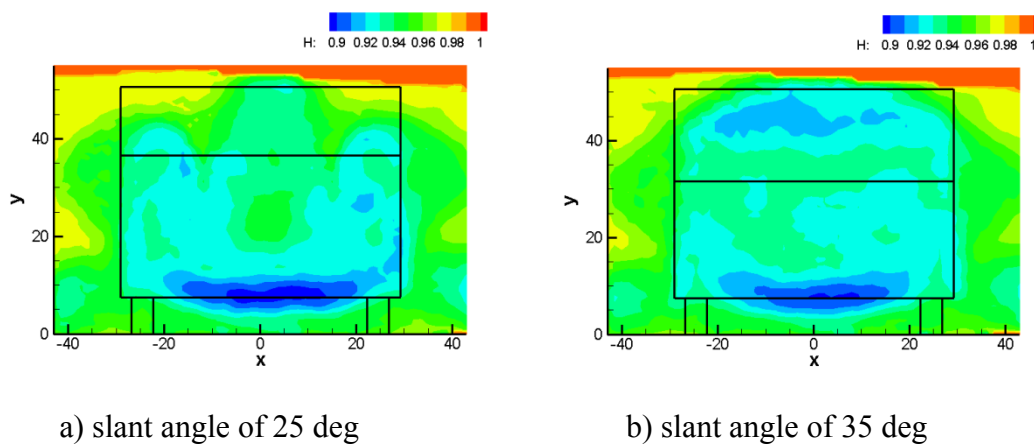


Fig. 15 – POD entropy distribution

Conclusions

The upper part of the wake forming a free shear layer was studied in detail. Two variants of the model with slant angles 25 deg and 35 deg were examined respectively. Angle 25° shows more or less attached flow, while angle 35 deg generates fully detached flow from the ramp. Maximal flow dynamical activity is located close to the road (wall), where for the 25 deg case quasiperiodical behaviour was detected.

References

- Ahmed S.R., 1981, Wake Structure of typical automobile shapes. Transactions of the ASME, Journal of Fluids Engineering, 103, 162-169, 1983.
- Ahmed, S.R., Ramm, G., 1984, Some Salient Features of the Time-Averaged Ground Vehicle Wake. SAE Technical Paper 840300.
- Ahmed, S.R., 1983, Influence of base slant on the wake structure and drag of road vehicles. Transactions of the ASME, Journal of Fluids Engineering V105, P429-434.
- Lienhart, H., Stoots, C., Becker, S., 2000, Flow and Turbulence Structures in the Wake of a Simplified Car Model (Ahmed Model), DGLR Fach Symp. der AG STAB, Stuttgart University, 15-17 Nov., 2000.

Ceyrowsky T., Brucker Ch., Schwarze R., 2009, Unsteady RANS Simulations of Flows Around a Simplified Car Body, EUROMECH COLLOQUIUM 509 Vehicle Aerodynamics External Aerodynamics of Railway Vehicles, Trucks, Buses and Cars, Berlin, Germany, March 24–25, 2009, pp.5-14.

Franck, G. & D'Elia, J., 2004, CFD modeling of the flow around the Ahmed vehicle model. In Proceedings of 2nd conference on advances and applications of GiD. Barcelona, Spain, 4p.

Lienhart, H., Stoots, C., Becker, S., 2000, Flow and Turbulence Structures in the Wake of a Simplified Car Model (Ahmed Model), DGLR Fach Symp. der AG STAB, Stuttgart University, 15-17 Nov., 2000.

Gilliéron P., Chometon F., 1999, Modelling of Stationary Three-Dimensional Separated Air Flows around an Ahmed Reference Model, ESAIM: Proc. 7, P173-182.

Uruba V., Sedlák K., 2009, Flow around Ahmed Body, Conference TOPICAL PROBLEMS OF FLUID MECHANICS 2009. Praha, Ústav termomechaniky AV ČR, v. v. i., 2009 - (Příhoda, J.; Kozel, K.) pp.107-110.

Uruba V., 2009, Dynamics of Flow in Wake behind Ahmed Body, Euromech Colloquium 509, Vehicle Aerodynamics: External Aerodynamics of Railway Vehicles, Trucks, Buses and Cars. Berlin: Herman-Fottinger-Institute TU Berlin, 2009 - (M.Schober; L.Lofdal; N.Nayeri) pp.236-247.

Acknowledgement

The authors gratefully acknowledge financial support of the Grant Agency of the Czech Republic, project No. 101/08/1112.